A R C H I V E S O F M E T A L L U R G Y A N D M A T E R I A L S
Volume 60 2015 Issue 3
DOI: 10.1515/amm-2015-0325

A. GOŁDASZ*,#, Z. MALINOWSKI*, T. TELEJKO*, A. BUCZEK*, M. RYWOTYCKI*, R. MARTYNOWSKI**, D. KOWALSKI**

THE DEVELOPMENT OF HEATING CURVES FOR OPEN DIE FORGING OF HEAVY PARTS

OPRACOWANIE KRZYWYCH NAGRZEWANIA ODKUWEK WIELKOGABARYTOWYCH

The study presents the findings of research on developing heating curves of heavy parts for the open die forging process. Hot ingots are heated in a chamber furnace. The heating process of 10, 30, 50 Mg ingots was analyzed. In addition, bearing in mind their high susceptibility to fracture, the ingots were sorted into 3 heating groups, for which the initial furnace temperature was specified. The calculations were performed with self developed software Wlewek utilizing the finite element method for the temperature, stress and strain field computations.

Keywords: charge heating, chamber furnace, finite element method.

W pracy przedstawiono wyniki badań dotyczących opracowywania krzywych nagrzewania odkuwek wielkogabarytowych przeznaczonych do kucia swobodnego. Proces nagrzewania gorących wlewków prowadzono w piecu komorowym. Analizowano proces nagrzewania wlewków 10, 30, 50 Mg. Dodatkowo mając na względzie dużą podatność na pękanie podzielono je na 3 grupy grzewcze, dla których wyznaczono początkową temperaturę pieca. Obliczenia wykonano Autorskim oprogramowaniem Wlewek służącym do obliczeń pola temperatury, naprężeń i odkształceń wlewków metodą elementów skończonych.

1. Introduction

As a result of an nonuniform temperature field forming in a heated or cooled material, strains and related thermal stresses occur. The material state is then described by three fields: temperature, strain and stress [1, 2]. As a result of a temperature increase, the volume changes due to a change in the material density. For some materials and temperature ranges the material structure changes as well. In processes with considerable temperature field nonuniformity, which can be caused by a high heating or cooling rate, or by the substantial weight of the charge, thermal stresses may reach values that can lead to fractures. For individual production of heavy components, fractures usually are non-removable defects and cause significant economic losses for the manufacturer.

The problem of calculating strains and stresses occurring in materials during the manufacturing processes is vital [3, 4]. In order to avoid defects caused by fractures, indicators that define acceptable thresholds of strains and stresses that do not cause the occurrence of fractures are determined. These indicators are called fracture criteria [5-7]. To determine these criteria one needs information on the stress and strain field occurring in the heated or cooled material, caused by the temperature field [8, 9]. Information on the temperature within the heated charge, which is the only one amongst the parameters discussed that can be directly measured, constitute the basis for the correct manufacturing process. As it is impossible to directly check the temperature inside the charge under the process conditions, the charge is heated on the basis of temperature measurements at the selected points of the furnace chamber by constructing heating curves.

2. Heat transfer model

To determine the temperature changes of the heated charge, the solution of the heat conduction equation with the finite element method was applied [10]:

$$\lambda\left[\frac{\partial^2 T}{\partial r^2}+\frac{1}{r}\frac{\partial T}{\partial r}+\frac{1}{r^2}\frac{\partial^2 T}{\partial \theta^2}+\frac{\partial^2 T}{\partial z^2}\right]+\dot{q}_V=\rho c\frac{\partial T}{\partial \tau} \qquad (1)$$

where:
- λ – heat transfer coefficient, W/(m·K);
- ρ – density, kg/m^3;
- c – specific heat, J/(k·gK);
- $\dot{q}_V$ – efficiency of the internal heat source, W/m^3;
- τ – time, s;
- r, z – cylindrical coordinates, m.

* AGH UNIVERSITY OF SCIENCE AND TECHNOLOGY, AL. MICKIEWICZA 30, 30-059 KRAKÓW, POLAND
** CELSA HUTA OSTROWIEC SP. Z O.O., 2 SAMSONOWICZA STR., 27-400 OSTROWIEC ŚWIĘTOKRZYSKI, POLAND
# Corresponding author: agoldasz@metal.agh.edu.pl

To describe the heat transfer in a chamber furnace, a simplified heat flow model was applied, where the furnace chamber is treated as a closed system comprising of two isothermal surfaces and an isothermal gas body (Fig. 1).

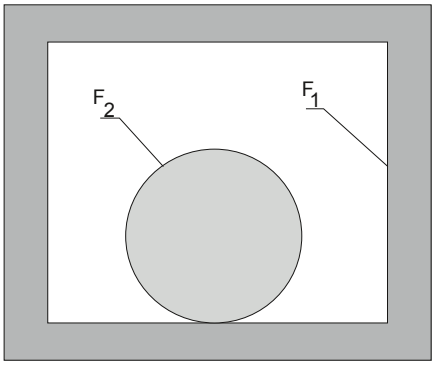

Fig. 1. A chamber furnace diagram applied in the boundary condition model for ingot heating: F_1 - furnace walls, F_2 - charge surface.

The isothermal surfaces are formed by the charge surface F_2 and furnace walls F_1. It was assumed in the model that the density of gas emissions reaching both surfaces is the same, and the transparency of the gas body for the wall radiation reaching the charge is the same as that of the wall radiation reaching the walls. It follows from the energy balance for the furnace chamber that the density of heat flux absorbed by the charge is:

$$q_2 = \frac{1}{1 - R_2 P_{g2}(\varphi_{22} + R_1 P_{g1}\varphi_{21})} \cdot \{e_g \varepsilon_2 (1 + R_1 P_{g1}\varphi_{21}) + e_1 \varepsilon_2 P_{g1}\varphi_{21} - e_2[1 - P_{g2}(\varphi_{22} + R_1 P_{g1}\varphi_{21})]\} + \alpha_k (T_g - T_2) \quad (2)$$

gdzie:

$\varphi_{21}, \varphi_{22}$ – average configuration coefficients,
F_1, F_2 – furnace and charge wall surface area, m^2
ε_2 – charge emissivity,
e_1, e_2 – density of own emission of wall and charge surface, W/m^2
P_{g1}, P_{g2} – transparency of the gas body radiation onto the charge and furnace wall surfaces,
R_1, R_2 – furnace and charge wall surface reflexivity,
α_k – convective coefficient of heat penetration at the charge surface, W/(m^{2}K)
T_g, T_2 – absolute temperature of the furnace atmosphere and charge surface, K.

The method of determination of average configuration coefficients and other parameters occurring in the formula (2) is presented in papers [11-13]. It was assumed that the combustion gases contain two radiating gases: CO_2 and H_2O.

The convective heat transfer coefficient at the charge surface was determined according to the formula [11]:

$$\alpha_k = 2{,}12(T_g - T_1)^{0{,}12} + \frac{(T_g - T_1)^{0{,}25}}{T_g L} \quad (3)$$

where:

T_1 − absolute temperature of the furnace walls, K
L − average length of the furnace wall, m

In order to connect the furnace wall temperature T_1 to the flue gas temperature, the following equation was applied:

$$T_1 = T_g - 5{,}67 \frac{1 - \varphi_{12}}{\alpha_{g1}} \frac{\varepsilon_1 \varepsilon_2}{\varepsilon_1 + \varphi_{12}\varepsilon_2(1 - \varepsilon_1)} \left[\left(\frac{T_1}{100}\right)^4 - \left(\frac{T_2}{100}\right)^4\right] \quad (4)$$

where:

ε_1 – furnace wall emissivity,

The heat transfer coefficient gas – furnace wall was determined with the formula

$$\alpha_{g1} = 5{,}67 \frac{\varepsilon_g}{T_g - T_1} \left[\left(\frac{T_g}{100}\right)^4 - \left(\frac{T_1}{100}\right)^4\right] \quad (5)$$

where:

ε_g – combustion gases emissivity,

The overall heat transfer coefficient of the charge was determined from the formula:

$$\alpha_2 = \frac{q_2}{T_p - T_2} \quad (6)$$

The furnace temperature is identified as T_p, and calculated as the arithmetic mean of the furnace wall temperature T_1 and the flue gas temperature T_g, which should be used for carrying out the ingot heating process.

3. Stress and strain model

In the heated ingots, thermal stresses develop, caused by an irregular temperature field and phase transitions occurring during heating. These stresses may lead to elastic or plastic strains. If the limit material formability has been exceeded, existing voids develop, local fractures form, and in extreme cases the ingot cracks. Nowadays, there are methods that enable the stress and strain field in materials subjected to thermal loads to be determined. The finite element method was applied to determine the stress and strain fields in ingots heated in the chamber furnace. The individual stages of the solution are as follows:

- expressing the displacement field {D} as a function of node displacements {Δ}. To define this field, the shape function must be determined.
- expressing the strain field {ε} as a function of the node displacement vector, by differentiating the displacement field in accordance with the definition of the small elastic-plastic strain tensor,
- defining the relationship between stresses and strains and expressing the stresses as a function of node degrees of freedom,
- defining the relationship between the forces in nodes and stresses from the condition of equilibrium between the node force power and stress power inside the element.

Due to the possibility of occurrence of plastic strains and time-variable heating conditions, the incremental method was used to determine the stress field, and the relationships between the stress and strain increments were defined with the Prandtl-Reuss equation. The methodology of determination of the stress and strain field was specified in the study [2].

4. Numerical calculations

Numerical simulations were conducted for the forging process of ingots Q10, Q30 and Q50 manufactured in industrial conditions. The heating process of hot ingots conducted in a chamber furnace with dimensions: 4m height, 5m width and 9m length was analyzed. Each time, the initial temperature of the ingot was determined taking into account the actual casting time, time taken to solidify in the mould and transport to the furnace. For each type of ingot, on the basis of preliminary numerical tests, three steel groups were selected, for which the initial furnace temperature was specified. The susceptibility of steel to fracture, in the form of a logarithmic strain [1] at the temperature of 500°C, was selected as the criterion for division of steels into groups:

- group I - acceptable logarithmic strain $\varphi_f = 0.07$,
- group II - acceptable logarithmic strain $\varphi_f = 0.06$,
- group III - acceptable logarithmic strain $\varphi_f = 0.04$.

For individual steel groups the initial furnace temperature was determined at which hot ingots are charged:

- group I - 1050°C,
- group II - 950°C,
- group III - 850°C.

Calculations were conducted for the selected steel grades, one per heating group. The chemical composition of steels is presented in table 1. The accuracy of numerical calculations largely depends on the physical and chemical properties of the material heated. The dependency of the heat conductivity coefficient on temperature is presented in Fig. 2; similarly, the values for specific heat are presented in Fig. 3.

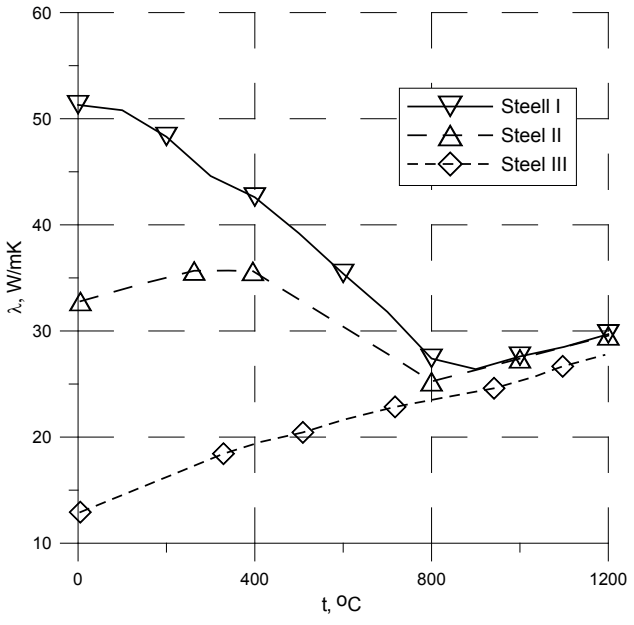

Fig. 2. Heat conduction coefficient [2]

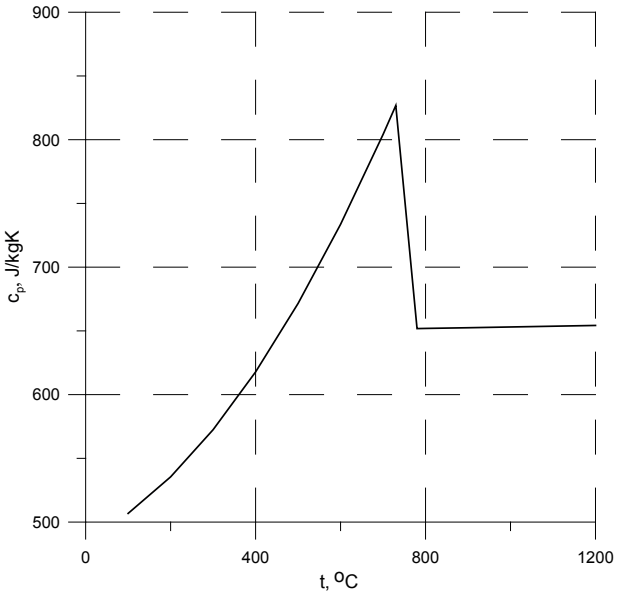

Fig. 3. Specific heat [2]

TABLE 1.

Chemical composition of steels

group	C	Mn	Si	Cr	Ni
	[%]				
Steel I	0,18	1,0	-	0,9	-
Steel II	0,34	0,55	0,27	0,78	3,5
Steel III	1,22	13	0,22	-	-

The subsequent figures present the results of numerical calculations for the process of ingot heating with a weight of 10 Mg (Q10), 30 Mg (Q30) and 50 Mg (Q50). Fig. 4 presents the developed heating curve for ingot Q10.

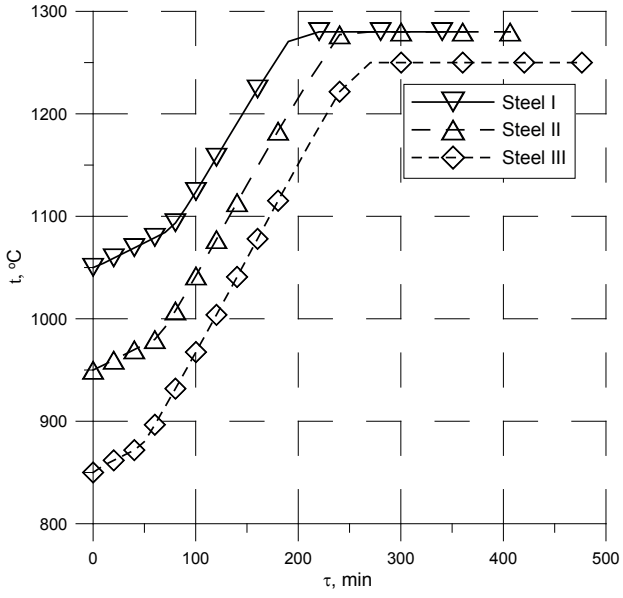

Fig. 4. The furnace chamber temperature distribution for heating an ingot of 10 Mg in weight

The overall heating time was 6 hours for steel I, 6.7 hours for steel II and 8 hours for steel III respectively. The maximum temperatures of the furnace chamber were assumed at the level of 1280°C for steels I and II, and 1250°C for steel III. The lower value of the furnace temperature arises from the much higher susceptibility to fracture of the steel grade analyzed when compared to the first two. A sufficiently long holding time ensured the desired temperature gradient in the ingot cross-section after completion of the heating (Fig. 5). For heating of the ingot of steel I and II, the temperature distribution after the completion of the process was identical. The temperature difference in the ingot cross-section did not exceed 80°C and was acceptable from a hot metal forming process perspective. The surface temperature may slightly exceed the forging temperature for individual steels, but this pertains only to zones located in the area of the ingot's foot and head. Thanks to the much longer heating time of steel III, the temperature difference does not exceed 60°C in the entire ingot volume (Fig. 5c). The maximum temperatures are located at the ingot surface and slightly exceed the forging temperature within the ingot head and foot areas.

For the calculation variant analyzed, the distribution of the effective logarithmic strain and average stress after completion of heating are also presented, Fig. 6-7.

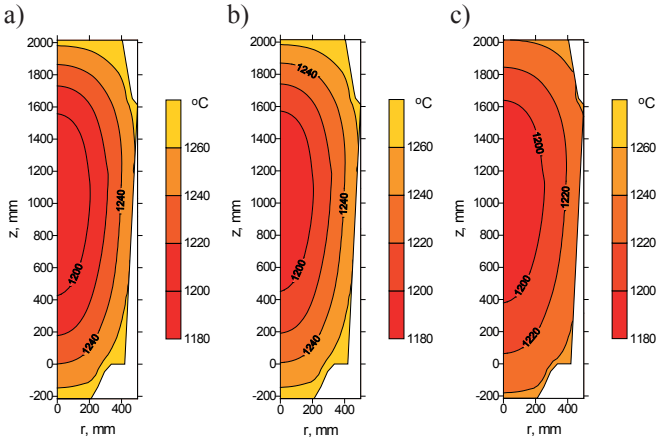

Fig. 5. The temperature distribution in the cross-section of the Q10 ingot heated: a) steel I, b) steel II, c) steel III

The effective logarithmic strain does not exceed a value of 0.004 in the ingot axis for all steel grades analyzed, Fig. 6. Higher values of the effective logarithmic strain were observed in the zone above 0.20 m towards the ingot radius; those values often exceeded 0.008. Bearing in mind that the average stress in the entire volume of the material heated does not exceed -10 MPa and is negative (compressive) this should be considered acceptable (Fig. 7).

Also calculations for much heavier ingots, which required longer heating times, were conducted. Fig. 8 presents the developed heating curves for ingots Q30. The heating times are: 10.7 h (steel I), 11.3 h (steel II) and almost 13 h for steel III. Compared to the Q10 ingot heating variant, the holding time at the maximum furnace chamber temperature has increased considerably.

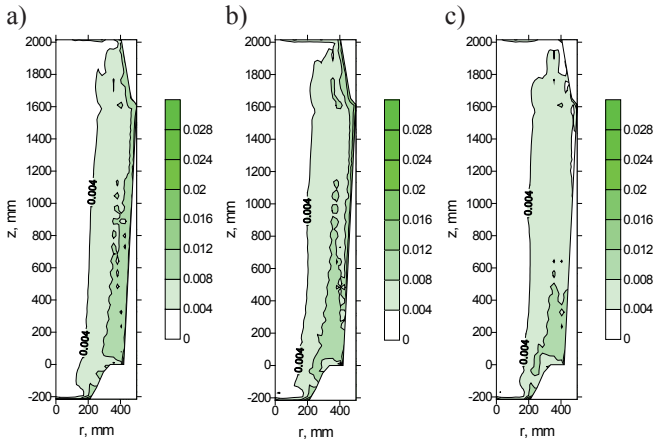

Fig. 6. The distribution of the effective logarithmic strain in the cross-section of the Q10 ingot heated: a) steel I, b) steel II, c) steel III

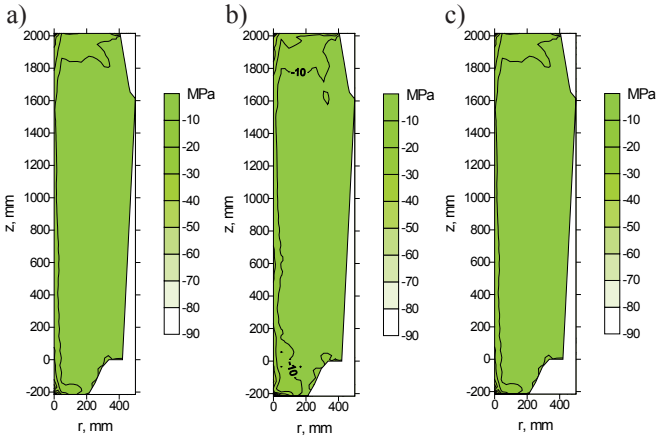

Fig. 7. The average stress distribution in the cross-section of the Q10 ingot heated: a) steel I, b) steel II, c) steel III

This resulted from the much larger weight, and thus also the ingot dimensions. The distribution of temperature, effective logarithmic strain and average stress in the cross-section of ingot Q30 after completion of heating is also presented. Due to substantial analogies in the distribution of individual values of parameters analyzed, the heating process of steel III is presented, taking into account its particular susceptibility to fracture, Fig. 9.

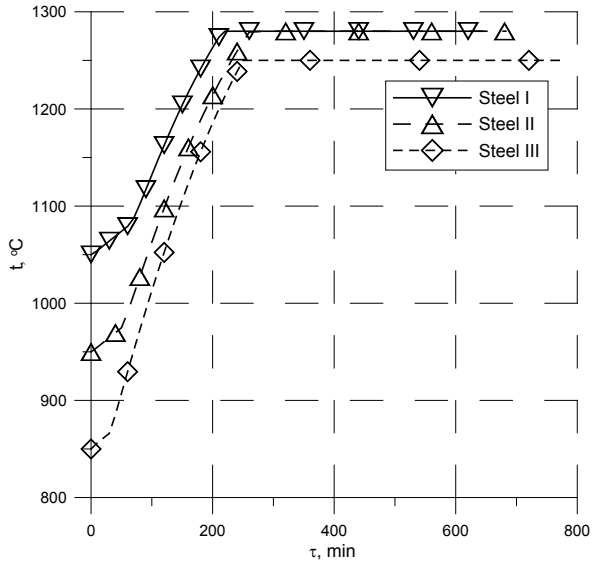

Fig. 8. The furnace chamber temperature distribution for heating of an ingot with a weight of 30 Mg

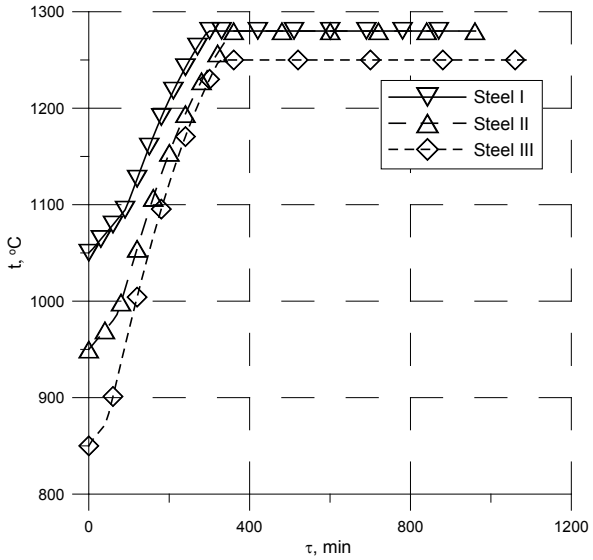

Fig. 10. The furnace chamber temperature distribution for heating of an ingot with a weight of 50 Mg

The effective logarithmic strain reaches values exceeding 0.012 only in the surface zone located near the foot and head of the Q30 ingot. The average stress value does not exceed -10MPa and in the entire volume it is compressive.

Also the heating process of ingots with a weight of 50 Mg was analyzed. Fig. 10 presents the furnace chamber temperature distribution; Fig. 11 the distribution of individual parameters for steel III. In this case also, the time of temperature rise to the holding temperature for all steel groups was extended. The overall heating time of the steel III ingot slightly exceeded 18 h. As for the Q10 and Q30 ingots, the desired temperature distribution after completion of heating was accomplished, Fig. 11. The logarithmic strain intensity assumes maximum values not exceeding 0.012, however in this case the average stress is positive (tensioning). The value of average stress does not exceed 10MPa and is located mainly in the ingot surface zone.

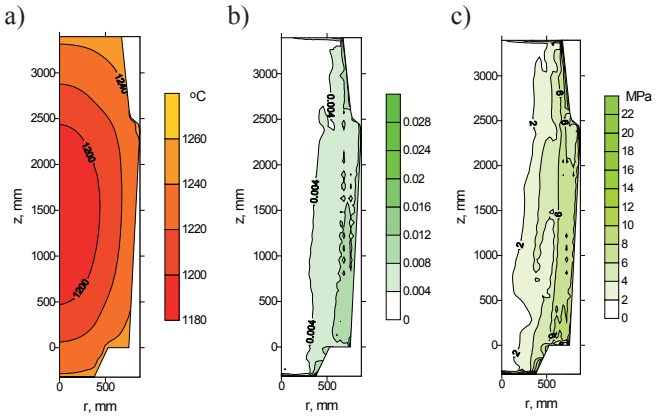

Fig. 11. The distribution of individual parameters in the cross-section of the Q30 -steel III ingot heated: a) temperature, b) effective logarithmic strain , c) average stress

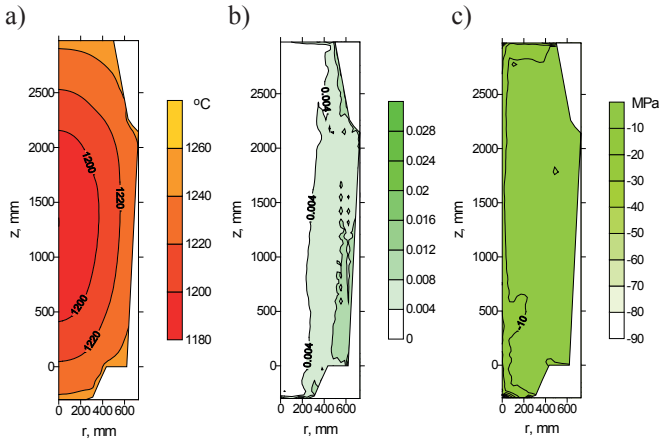

Fig. 9. The distribution of individual parameters in the cross-section of the Q30 -steel III ingot heated: a) temperature, b) effective logarithmic strain , c) average stress.

5. Conclusion

In this project, the self developed software that allowed a quick (a few minutes) analysis of the heating process of ingots for open die forging was applied to construct furnace chamber temperature curves. The heat transfer model takes into account both radiation and convection, which, with the current tendency to replace the ceramic lining in furnaces with fibrous lining, ensures high accuracy of the numerical simulation results.

Developing heating curves for heavy ingots should be performed in conjunction with the analysis of the strain and stress state of the material tested. Such a comprehensive approach allows one to use as short ingot heating times as possible, taking their susceptibility to fracture into account. A complete analysis of the formation of material defects would require conducting a static tensile test, which is a source of necessary information for fracture criteria.

When determining heating curves, low heating rates were applied, taking into account the highest possible furnace

temperature. This involves an extension of the furnace chamber temperature increase stage, but also reduces the power that is necessary to ensure the obtained heating curve. Also the holding time of ingots at the temperature specified by the forging process is shortened. Bearing in mind that the heating time for the heaviest ingots may reach as much as 18 hours, the approach to designing heating curves presented in this paper will result in as low gas consumption as possible, while ensuring the superior quality of the final product.

Final note: The project was financed under the Gekon Programme – the Environmentally Friendly Concept Generator. Project No. GEKON1/O2/213082/4/2014

REFERENCES

[1] B. Hadała, A. Cebo-Rudnicka, Z. Malinowski, A. Gołdasz, Archives of Metallurgy and Materials **56**, 367 (2011).
[2] Z. Malinowski, Numeryczne modele w przeróbce plastycznej i wymianie ciepła. Kraków (2005).
[3] W. Piekarska, M. Kubiak, Z. Saternus, Archives of Metallurgy and Materials **57**, 1219 (2012).
[4] W. Piekarska, M. Kubiak, Z. Saternus, Rek K., Archives of Metallurgy and Materials **58**, 1237 (2013).
[5] M. Morawiecki, L. Sadok, E. Wosiek, Przeróbka plastyczna. Podstawy teoretyczne. Katowice (1986).
[6] R.H. Wagoner, J.L. Chenot, Metal forming analysis. Cambridge University Press (2001).
[7] S. Kobayashi, S. Oh, T. Altan, Metal forming and the finite element method. Oxford University Press (1989).
[8] M. Norris, J. E. Reaugh, B. Moran, D.F. Quinones, Trans. ASME Journal of Engineering Materials and Technology **100**, 279 (1978).
[9] W.M Garrison., N.R. Moody, Journal of Physics and Chemistry of Solids **48**, 1035 (1987).
[10] S. Wiśniewski, T. Wiśniewski, Wymiana ciepła. WNT 1997.
[11] Z. Malinowski, J.G. Lenard, M.E. Davies, Journal of Materials Processing Technolog **41**, 125 (1994).
[12] E. Kostowski, Promieniowanie cieplne. PWN (1993).
[13] A. Gołdasz, Z. Malinowski, T. Telejko, M. Rywotycki, A. Szajding, Archives of Metallurgy and Materials **57**, 1143 (2012).

Received: 20 January 2015.